Somatostatin Receptor Imaging and Theranostics: Current Practice and Future Prospects

Authors

Sonya Park[1] (park@catholic.ac.kr)

Ashwin Singh Parihar[2] (ashwinsinghparihar@gmail.com)

Lisa Bodei[3] (bodeil@mskcc.org)

Thomas A Hope[4] (Thomas.Hope@ucsf.edu)

Nadine Mallak[5] (mallak@ohsu.edu)

Corina Millo[6] (millocm@cc.nih.gov)

Kalpna Prasad[7] (Drkalpna2000@gmail.com)

Don Wilson[8] (DWilson@bccancer.bc.ca)

Katherine Zukotynski[9] (zukotynk@mcmaster.ca)

Erik Mittra[5*] (mittra@ohsu.edu)

Affiliations

Departments of [1]Nuclear Medicine, Seoul St. Mary's Hospital, Seoul, Korea; [2]Nuclear Medicine, Postgraduate Institute of Medical Education and Research, Chandigarh, India; [3]Molecular Imaging and Therapy Service, Memorial Sloan Kettering Cancer Center, New York, NY, USA; [4]Radiology and Biomedical Imaging, University of California San Francisco, San Francisco, USA; [5]Diagnostic Radiology, Oregon Health & Science University, Portland, OR, USA; [6]Nuclear Medicine, RAD&IS; Clinical Center, National Institutes of Health, Bethesda, MD, USA; [7]Nuclear Medicine, Walter Reed National Military Medical Center, Bethesda, MD, USA; [8]BC Cancer, Vancouver, British Columbia, Canada, and [9]Radiology and Medicine, McMaster University, Hamilton, Ontario, Canada.

Word Counts

Total words: 6301

Table: 1

Figures: 9 (5 main, 4 supplementary)

First Author

Sonya Park

Department of Nuclear Medicine, Seoul St. Mary's Hospital, Seoul, Korea

Tel: +82 (2) 2258-1550; Email: park@catholic.ac.kr

Corresponding Author

Erik Mittra, MD, PhD

Department of Diagnostic Radiology, Division of Nuclear Medicine & Molecular Imaging, Oregon Health & Science University, 3181 SW Sam Jackson Park Rd., Mail Code L340, Portland, OR, 97239, USA

Tel: (503) 494-4974; Email: mittra@ohsu.edu

Running Title

Somatostatin receptor theranostics

Noteworthy points:

1. SSTR-PET can be used to reliably assess SSTR expression both visually and semi-quantitatively. (p10)

2. SSTR-PET is essential for the proper assessment of eligibility for PRRT. (p11)

3. SSTR expression is both a prognostic (correlates with outcome regardless of the therapy) and predictive (correlates specifically with response to PRRT) parameter for NENs. (p13)

ABSTRACT

A new era of precision diagnostics and therapy for patients with neuroendocrine neoplasms began with the approval of somatostatin receptor (SSTR) radiopharmaceuticals for positron emission tomography (PET) imaging followed by peptide receptor radionuclide therapy (PRRT). With the transition from SSTR-based gamma scintigraphy to PET, the higher sensitivity of the latter raised questions regarding the direct application of the planar scintigraphy-based Krenning score for PRRT eligibility. Also, to date, the role of SSTR-PET in response assessment and predicting outcome remains under evaluation. In this comprehensive review article, we discuss the current role of SSTR-PET in all aspects of neuroendocrine neoplasms including its relation to conventional imaging, selection of patients for PRRT, and the current understanding of SSTR-PET based response assessment. We also provide a standardized reporting template for SSTR-PET with a brief discussion.

Key-words

INTRODUCTION

Neuroendocrine neoplasms (NENs) are rare, heterogeneous, and typically slow-growing, accounting for ~0.5% of all diagnosed malignancies. Originating from the secretory cells of the neuroendocrine system at almost any anatomic site, their site of origin is often linked to disease biology. For example, tumors of the ileum typically have a high malignant potential, although metastatic lesions tend to have an indolent course. Gastric and rectal tumors have a low metastatic potential but can grow aggressively once metastatic (*1*). Gastro-entero-pancreatic, pulmonary, and thymic NENs are among the most-commonly diagnosed (*2*). The term NENs encompasses both well-differentiated neuroendocrine tumors (NETs) and poorly differentiated neuroendocrine carcinomas (NECs). Whereas NECs are high grade by default, NETs are classified further according to histologic grade and degree of differentiation, with site-specific parameters (cut-offs). Grading for gastro-entero-pancreatic NETs, for example, is based on proliferation using either the Ki-67 index or mitotic count per 10 high-power-fields (HPFs). Grade-1 (G1 or low-grade) refers to Ki-67 of <3% and <2 mitoses/10HPF, G2 refers to Ki-67 of 3-20% or 2-20 mitosis/10HPF, and G3 refers to Ki-67 of >20% or >20 mitoses/10HPF (*3*). Based on the degree of differentiation they are categorized as either well-differentiated or poorly differentiated tumors. Most NENs are sporadic, although some arise in the setting of inherited syndromes such as Multiple Endocrine Neoplasia, Tuberous Sclerosis, Von-Hippel-Lindau disease, or Neurofibromatosis (*1*).

NENs typically have increased expression of somatostatin receptors (SSTRs), G-protein coupled receptors modulating cellular proliferative and secretory activity. This forms the basis of functional imaging with SSTR targeting radiopharmaceuticals and treatment with somatostatin

analogues (SSAs) including octreotide and octreotate. There are five sub-types of SSTRs with sub-types 2, 3 and 5 most commonly expressed (*4*). [111]Indium- diethylenetriamine pentaacetate (DTPA)-conjugated octreotide (^{111}In-pentetreotide/ OctreoScan) was the first agent to receive United States Food and Drugs Administration (FDA) approval in 1994 for functional imaging of NENs with planar scintigraphy or single-photon emission computed tomography (SPECT) (*5*). ^{99m}Tc-labeled somatostatin analogs, including the commercially available ^{99m}Tc-Ethylenediaminediacetic acid Hynic-[D-Phe1, Tyr3-Octreotide] (^{99m}Tc-EDDA-Hynic-TOC), were also developed to improve image quality with lower radiation absorbed dose (*6*). Newer [68]Ga- or [64]Cu- tetraxetan (DOTA)-conjugated SSAs for positron emission tomography (PET) have shown superior diagnostic performance compared to ^{111}In-pentetreotide and are the current modality of choice for functional imaging (*5,7*). Different DOTA-peptides exist and have varying affinity for the SSTR subtypes (Table 1).

Management of NENs is based on the grade, subtype, distribution, and extent of disease. Anatomic imaging with computed tomography (CT) and magnetic resonance imaging (MRI) is standard practice to assess disease location and extent, although radiopharmaceutical development has led to improvements in imaging and therapy (together termed theranostics). Initially, high dose ^{111}In-pentetreotide was used for therapy (*8*), via Auger electrons, although the efficacy was limited (*9*). The use of [177]Lutetium or [90]Yttrium (beta-emitters), conjugated to SSAs with DOTA has been more effective (*10*). Specifically, ^{177}Lu-DOTA-Tyr^3-octreotate (DOTATATE) based PRRT studied in a phase 3, multicenter, randomized control trial (NETTER-1) in patients with inoperable or advanced and progressive midgut NENs, showed superior outcomes in comparison to standard-of-

care therapy *(10)*.

This paper reviews the current status and advances in imaging of NENs, with a focus on the use of SSTR-PET with respect to PRRT.

THE ROLE OF CONVENTIONAL IMAGING

CT is commonly the initial imaging modality for evaluation of a suspected NEN. The detection rate of primary small bowel NENs is ~50% (*11,12*). Metastatic mesenteric nodes are typically larger than the primary itself and are often calcified. When a small bowel NEN is known or suspected, a negative oral contrast (methylcellulose, polyethylene glycol, or water) is preferred over conventional radiopaque contrast, to avoid masking the primary enhancing lesion on the bowel wall (*13,14*). Primary pancreatic NENs (pNENs) have a detection rate of ~80-100% on CT (*15*). It is important to obtain an abdominal multiphase CT with IV contrast, since most pNENs and their hepatic metastases are arterially enhancing and occult on a single portal venous phase (*11,14,16*) (Figure 1). Around 22% of pNENs are arterially hypo-enhancing, where the portal venous and delayed phases can help in detection (*11,17*).

MRI is superior to CT for detecting hepatic metastases (*18,19*). As with CT, multiphase MR imaging with IV contrast is recommended since most primary and metastatic NENs show arterial enhancement. Additionally, Diffusion Weighted Imaging (DWI) and delayed post-contrast phase using Gadoxetic acid (hepato-specific paramagnetic contrast agent) are useful for detection

of hepatic metastases. Hepatic metastases typically show high signal on DWI (combination of T2 shine-through and true diffusion restriction), which makes them more conspicuous; this tool is especially helpful in patients with severe renal failure where IV gadolinium is contraindicated (*19,20*). The most sensitive tool for detection of hepatic metastases is the 20-minutes post-contrast delayed phase after IV administration of Gadoxetic acid (Figure 2), which is retained in hepatocytes but not in metastases, creating a high lesion-to-background contrast on the delayed image. In addition to having high sensitivity for lesion detection, the 20-minute delayed phase allows for more accurate and reproducible measurement of baseline and follow-up lesion dimension on imaging (*20-23*).

Findings on anatomic imaging associated with higher grade tumors, which apply to both CT and MRI include: large tumor size (≥2 cm), ill-defined margins, low/ moderate arterial hyper-enhancement, dilatation of the main pancreatic duct, vascular invasion, and presence of nodal/ distant metastases; findings specific to MRI include non-intense T2 signal, and most importantly, high diffusion restriction (*24,25*). Several studies show that ADC values inversely correlate with mitotic-count and Ki-67 index. A significant difference in ADC values has been observed between G1 and G2 tumors and between G1/G2 and G3 tumors, with suggested cutoff ADC values below 0.95×10^{-3} to 1.19×10^{-3} mm^2/s for G3 tumors (18,19).

PET RADIOPHARMACEUTICALS

Introduced in 2001, ^{68}Ga-DOTATOC (DOTA-Tyr^3-octreotide) was the first PET-SSA ligand (*26*). As opposed to the SSTR2-selective DOTATATE, DOTATOC retains an octreotide-

like affinity profile (Table-1) (*27*). A comparison of ^{68}Ga-DOTATOC to ^{68}Ga-DOTATATE PET/CT in the same patients showed a similar diagnostic accuracy, despite potential advantages for ^{68}Ga-DOTATOC in the total number of detected lesions and a higher Standardized Uptake Value maximum (SUVmax) (*28*). Today, ^{68}Ga-DOTATOC and ^{68}Ga-DOTATATE are the most commonly used radiopharmaceuticals for imaging NENs, with no clear superiority of either one of these compounds.

One of the main disadvantages of ^{68}Ga-SSA-based imaging is the high liver background and short radiopharmaceutical half-life. For the latter, newer SSTR radiopharmaceuticals, such as Copper-64 (^{64}Cu) labeled-SSA (FDA-approved in September 2020) may provide an advantage. Figure 3 shows the same patient imaged with the two different radioisotopes. Potential advantages of ^{64}Cu include its longer half-life (12.7 hours versus 68 minutes for ^{68}Ga) and resultant higher target-to-background ratios on delayed imaging, as well as shorter positron range in tissue (mean 0.6 mm versus 3.5 mm for ^{68}Ga). These factors may result in better imaging characteristics, especially at later times (3-24 hrs post-injection) (*29*). Conversely, ^{64}Cu has a significantly lower positron branching-ratio(0.17) than ^{68}Ga (0.89) which may degrade image quality or at least require a longer acquisition time. A prospective head-to-head comparison of ^{64}Cu-DOTATATE and ^{68}Ga-DOTATOC PET/CT in 59 subjects with NENs showed ^{64}Cu-DOTATATE to be advantageous, detecting 83% of the true-positive lesions which were discordant between the radiopharmaceuticals (*30*). However, dual time-point imaging with ^{64}Cu-DOTATATE in 35 patients showed similar accuracy for 1-hour and 3-hour imaging (*31*), suggesting that the improved detection rate seen in the previous study was due to factors other than the target-to-background

9

ratio. Notably, ^{64}Cu-DOTA is prone to demetallation and transchelation in vivo, and better results may be expected with new sarcophagine based chelators (*32*).

The SSAs discussed thus far are SSTR-agonists, resulting in activation and internalization of the receptor upon binding. Radiolabeled SSTR antagonists, such as ^{68}Ga-DOTA-JR11, are characterized by a lack of internalization, rapid blood-pool clearance, and greater tumor uptake, aiding detection of metastases (*33*). A prospective head-to-head comparison between ^{68}Ga-NODAGA-JR11, a SSTR antagonist, and ^{68}Ga-DOTATOC PET/CT in 12 patients of NENs demonstrated that the favorable biodistribution of the antagonist resulted in a higher detection rate of hepatic metastases and a significantly greater lesion-based overall sensitivity (94% vs. 59%) (*34*).

In cases where SSTR imaging is suboptimal, other PET agents have been developed to target different receptors overexpressed by the NENs, including the GLP-1 (Glucagon-like-Peptide 1) receptor ligand ^{68}Ga-DOTA-Exendin-4, which may facilitate the detection of benign insulinomas (frequently SSTR-negative) (*35,36*). The CXCR-4 ligand ^{68}Ga-Pentixafor seems superior to conventional SSTR imaging for G3 NETs, but its role relative to ^{18}F-FDG PET remains to be determined (*37*). SSTR-PET typically shows high uptake in well-differentiated or low-grade lesions, and lower uptake in poorly differentiated or high-grade lesions. In the latter scenario, ^{18}F-FDG PET is complementary in that it detects aggressive, poorly differentiated disease with higher grade and worse prognosis (Figure 4, Supplementary Figures 1, 2). Around 40% of patients or less with G1 disease are thought to have ^{18}F-FDG- uptake, while almost all patients with G3 disease

have ^{18}F-FDG uptake (*38-41*). Since NENs are vastly heterogeneous and it would be impossible to sample all lesions in the body, the combination of SSTR and ^{18}F-FDG PET provides a non-invasive understanding of disease heterogeneity and likelihood of PRRT response (*42*).

Currently, ^{18}F-FDG PET is used for staging G3 disease and can be used to complement SSTR-PET when Ki-67 is 10% or more (*41*). Also, a positive ^{18}F-FDG PET may be used to reconsider PRRT for a patient. Specifically, the combination of high SSTR, and low ^{18}F-FDG avidity, increases the likelihood of benefit from PRRT; however, the ratio of differentiated to de-differentiated disease at which PRRT ceases to be useful, remains to be determined. In fact, it seems possible that in the event of marked uptake on SSTR-PET with limited sites of ^{18}F-FDG-avid disease a combination of PRRT and targeted external radiation to the ^{18}F-FDG avid lesions may prolong survival. Ultimately, a combination of SSTR- and ^{18}F-FDG PET will likely provide a synergistic pictorial road-map of disease for determining when to use PRRT, combination PRRT and targeted external radiotherapy versus an alternative therapy (*43-45*).

TUMOR QUANTIFICATION, CURRENT GUIDELINES AND THE KRENNING SCALE

SSTR-PET can be used to assess SSTR expression visually and semi-quantitatively. Cell membrane–based SSTR2 expression on immunohistochemistry (IHC) in NENs correlates with the SUVs on ^{68}Ga-DOTATOC PET/CT (*46*). Some cases considered negative on IHC demonstrated mild uptake on SSTR-PET possibly due to SSTR-5 binding or tumor heterogeneity. Campana (*47*) suggested that the SUVmax correlated with clinico-pathologic features of NENs and could serve as a prognostic index, alongside anatomic location, primary tumor grade and Ki-67 status. Velikyan

(*48*) reported that kinetic modeling parameters, rather than SUV, reflected receptor density more accurately based on absence of a linear correlation between SUV and net uptake rate in tumors with high SSTR expression. Specifically, SUVs correlated with receptor density at low values, with a non-linear relationship thereafter leading to underestimation of receptor expression. While this might reflect plasma peptide availability as a limiting factor for tracer uptake in patients with high SSTR expression and high tumor burden, an alternative explanation could be related to receptor saturation.

More recently, volumetric parameters have been evaluated in well differentiated NENs (*49*). Specifically, the concept of SSTR Expressing Tumor Volume (SRETV), representing the volume of tumor with > 50% SUVmax uptake, and Total Lesion SSTR Expression (TLSSTRE) calculated as SRETV x SUVmean in the volume of interest have been defined. A sum of each of these volumetric parameters can be calculated; the literature suggests there may be a significant correlation between whole-body cumulative SRETV and PFS following PRRT. Nevertheless, estimation of tumor volume based on uptake will likely remain problematic given the intrinsic heterogeneity in tumoral SSTR expression.

Recent guidelines formulated under the auspices of the European Association of Nuclear Medicine recommend the use of ^{68}Ga-labelled somatostatin analogues in combination with CT or MRI for diagnosis, staging, restaging after surgery, following progression and for known or suspected NETs (*50*). The National Comprehensive Cancer Network guidelines recommend SSTR-PET prior to PRRT for advanced NENs (*51*). While a few studies using ^{68}Ga-DOTATOC

have suggested that SUVmax thresholds be used to determine eligibility for PRRT e.g. SUVmax cut-off 17.9 (*52*) and 16.5 (*53*), differences between scanners and imaging technique may produce slight variations which make SUVmax problematic to use. An alternative is to use a tumor:liver ratio of 2.2 (*53*). The American College of Radiology practice parameters suggest visually assessed tumor uptake equal to/ more than liver as an eligibility criteria for PRRT (*54*).

The Krenning score was developed using ^{111}In-pentetreotide scintigraphy (*8*) and has been extrapolated to SSTR-PET ('Modified' Krenning score). A 5-point scale has been proposed based on a qualitative assessment of lesion uptake relative to blood pool and hepatic activity where: 0-no uptake, 1-very low uptake, 2-uptake $\leq$ liver, 3-uptake > liver, and 4-uptake > spleen (*55*). However, the relationship between the Krenning score from ^{111}In-pentetreotide scintigraphy and the modified Krenning score from SSTR-PET is limited (*56*). Disease on SSTR-PET has a bias toward higher scores as compared to ^{111}In-pentetreotide scintigraphy (Supplementary Figure 3). Part of this is due to differences in equipment (higher sensitivity of PET versus planar-scintigraphy/ SPECT) and imaging time points (^{111}In-pentetreotide scintigraphy–24 hrs post-injection; SSTR-PET–1 hr post-injection).

While there is little formal data to support the use of SSTR-PET over ^{111}In-pentetreotide scintigraphy, SSTR-PET has become the standard for pre-PRRT patient selection because of its higher sensitivity, faster imaging times, and lower radiation dose. For lesions >2 cm, it is appropriate to use the modified Krenning Score and PRRT should be considered with a score of 3/4. Caution should be used before treating patients with lesions measuring <2 cm with a modified

Krenning Score of 3/4, as these patients are unlikely to have fulfilled criteria if imaged with ^{111}In-pentetreotide. This is to emphasize that the current data does not provide sufficient evidence for the use of SSTR-PET in this setting. PRRT should not be considered when lesions show no or low uptake on SSTR-PET.

REPORTING SSTR-PET

There is a need for standardized interpretation of SSTR-PET given that findings on baseline imaging in-part determine treatment success with radioligand therapies (*57*). The report (Supplementary Figure 4) should include a concise clinical history, including NEN subtype, tumor grade and differentiation, and prior treatments (medical/ surgical). The imaging parameters, in terms of the specific radiopeptide and its administered activity, uptake time, duration of imaging (time per-bed position) and area imaged, should be documented. Comparison and correlation with any prior SSTR-imaging, ^{18}F-FDG PET, and other anatomic imaging should be performed. Findings should detail the site and size of the lesion(s) (the latter if seen on corresponding CT/ MRI) and uptake intensity, which can be expressed semi-quantitatively (commonly as SUVmax). The pattern of tracer uptake (intra-lesional heterogeneity) and assessment of lesion resectability (i.e. relation with vascular and major structures) may be helpful to further guide management. The conclusion should provide the modified Krenning score and additional diagnostic examinations or follow-up can be suggested.

The "NETPET" score is a grading system that combines findings on SSTR and ^{18}F-FDG PET with a single parameter (*58*). This scoring system has been developed as a prognostic

biomarker. Although rarely included in reports since SSTR and ^{18}F-FDG PET are not routinely performed together, this may change in future.

The SSTR-reporting and data systems (RADS) has also been introduced as part of the umbrella *molecular imaging* (MI) *RADS*, a 5-point scale (from 1- no evidence of disease and definitely benign to 5- high certainty for NEN) indicating both disease site and radiotracer avidity (*55*). SSTR-RADS entails a 3-point qualitative assessment scoring of uptake level, where up to five target (largest, most avid) lesions can be identified, with overall score defined as the highest scored lesion. A summed RADS score, including all 5 target lesions, has also been suggested (*59*). Future validation of this framework is warranted, including inter- and intra-observer agreement studies and histopathology correlation.

Disease Burden, Outcome Prediction and Response Assessment

SSTR expression is both a prognostic (correlates with outcome regardless of therapy) and predictive (correlates specifically with response to PRRT) parameter for NENs. (*60*). The current literature suggests that higher baseline SUVs on SSTR-PET predict better post-PRRT outcomes. Oksuz (*52*) reported high pre-therapy primary tumor uptake suggested a good response to PRRT; Kratochwil (*53*) reported high pre-therapy uptake in liver metastases suggested a good response; and Ambrosini (*60*) reported better outcomes in patients with high baseline SUVs. To avoid scanner related variations, parameters such as tumor-to-liver (T/L) and tumor-to spleen ratios may be used. It has been reported that a T/L>2.2 is predictive of a favorable response. It has, however,

been demonstrated that a high uptake (e.g. Krenning grade 4) is associated with response to PRRT only in 60% of patients (*61*).

The literature on response evaluation is more variable, and we are still beginning to understand how post-therapy SSTR-PET correlates with end points such as time to progression (TTP), progression-free (PFS) and overall survival (OS). Haug et al. (*62*) studied SUVmax and T/S ratio for prediction of TTP and clinical outcome following a 1st PRRT cycle in well-differentiated NENs. The authors found that reduced uptake post-therapy predicted TTP and correlated with clinical improvement. Further, interval change in the T/S ratio was superior to interval change in SUVmax. Meanwhile, Gabriel (*6*) reported essentially random SUV fluctuations following PRRT. The question remains: Does diminishing tumoral radiotracer uptake reflect true disease improvement or is there a higher degree of tumor de-differentiation with loss of SSTR expression? Accordingly, the recently updated appropriate use criteria (*63*) for SSTR-PET notes that response assessment should be assessed by the disappearance of known lesions or development of new lesions, rather than changes in SUVs.

Monitoring response to PRRT with SSTR-PET and attempting to interpret the biologic significance of tumor uptake change is challenging. One study evaluated 46 patients with advanced NENs treated with 2-7 cycles of PRRT and compared the results from the post-therapy ^{68}Ga-DOTATATE PET to CT/ MRI with RECIST. The authors found little advantage of SSTR-PET over conventional imaging for response assessment (*6*). In another study of 66 patients, ^{68}Ga-DOTATOC and ^{18}F-FDG PET was done at baseline, at 3 months, and again at 6-9 months following

completion of PRRT. The authors concluded that uptake on ^{18}F-FDG PET at baseline and follow-up had a stronger correlation with the outcome than SSTR-PET, and that combination imaging with both radiopharmaceuticals might be advisable across all tumor grades (*43*).

Also, a high overall tumor burden and tumor heterogeneity on SSTR-PET, is likely to be associated with worse prognosis. SSTR-PET helps in assessing the heterogeneity of NENs that exists at the inter-patient, intra-patient, inter-lesional level at a specific time point or longitudinally at different time points. This heterogeneity implies a variety of cells displaying variable characteristics in terms of metabolism, proliferation, metastatic potential, and therapy response. Distinct metastases may harbor different cellular clones with varying SSTR expression. The primary tumor and its metastases may also differ. Indeed, this may impact the chance of PRRT success and explains why cure is rarely possible with systemic metastatic disease. In a study by Graf et al (*64*), only patients with at least 90% of metastases positive for SSTR were treated with PRRT. Positive lesions were viewed in 3 dimensions and a lesion that had a change in score from 3/4 to 2, or from 2 to 1 that persisted over >5 mm in any plane was defined as heterogeneous. Only the solid portion of a necrotic lesion was assessed. If >50% of lesions were deemed heterogeneous, the patient was labeled as heterogeneous. This study confirmed that heterogeneity had a negative impact on OS and TTP following PRRT. Indeed, heterogeneity surpassed Ki-67 as prognostic marker, especially related to PRRT, reinforcing the suspicion that PRRT may target the less aggressive, SSTR-positive cells, sparing the rest. Thus, even when decreased tumor size suggests response by RECIST criteria, the more aggressive cells might remain viable. These observations highlight an intrinsic flaw of using quantitative parameters such as SUVmax alone, which do not

account for the intralesional variation of SSTR expression. Interestingly, some authors have observed that, following PRRT, heterogeneous lesions may become more homogeneous. In future, use of textural characteristics such as entropy and skewness may prove superior to our current methodology for lesion analysis.

Recently, a prospective study in 158 patients divided in three independent ^{177}Lu-PRRT cohorts demonstrated that specific circulating tumor transcripts (mRNA) specifically predict the outcome of PRRT and therefore represent a marker of radiosensitivity (*65*), while the circulating transcript signature NETest allows accurate monitoring of the course of disease during treatment and integrates with imaging (*66*).

The primary site of the tumor, which can often be elucidated with SSTR-PET, is a prognostic factor and should be incorporated in the decision algorithm for PRRT. Midgut and pNENs are included in the FDA approved indications for PRRT. Bronchial NENs represent a special category with typical tumors considered more appropriate for PRRT due to higher SSTR expression. In the case of a pheochromocytoma or paraganglioma, the current recommendation reserves PRRT for MIBG negative tumors only, where ^{131}I-MIBG treatment is precluded. The distribution and extent of disease, ideally evaluated with SSTR-PET, also affects management. In general, caution is needed in tumors with extensive mesenteric and peritoneal involvement, since PRRT may increase complication risk from a desmoplastic reaction. As the tumors metastasize, the total tumor burden may play a role depending on the primary site of disease. For example, pancreatic NENs with >25% liver involvement and bone metastases have worse prognosis, while

gastric NENs show no significant difference in outcome based on distribution (*67*). In general, tumor burden is termed limited if <5 lesions are detected at one site; moderate if >5 lesions, at two sites; and extensive if >2 sites are involved, and this affects the treatment approach (Figure 5). Most gastro-entero-pancreatic NENs present with hepatic metastases at diagnosis despite low Ki-67 and the presence of hepatic metastases profoundly decreases OS. PRRT may be helpful for non-resectable hepatic metastases and indeed may render the lesions resectable. In liver dominant disease, intra-arterial PRRT is being investigated.

CONCLUSION

SSTR-PET is the preferred imaging modality at initial diagnosis of low- and intermediate-grade NENs especially for localization of the primary tumor and determining disease extent. It is essential for selecting patients for PRRT, while its role in response monitoring is still being evaluated. While SSTR expression can be assessed visually and semi-quantitatively, with various suggested thresholds, a modified Krenning score is used in current clinical practice.

DISCLOSURE

No potential conflicts of interest relevant to this article exist.

REFERENCES

1.   Cives M, Strosberg JR. Gastroenteropancreatic neuroendocrine tumors. *CA Cancer J Clin.* 2018;68:471-487.

2.   Rindi G, Klimstra DS, Abedi-Ardekani B, et al. A common classification framework for neuroendocrine neoplasms: an International Agency for Research on Cancer (IARC) and World Health Organization (WHO) expert consensus proposal. *Mod Pathol.* 2018;31:1770-1786.

3.   Nagtegaal ID, Odze RD, Klimstra D, et al. The 2019 WHO classification of tumours of the digestive system. *Histopathology.* 2020;76:182-188.

4.   Krenning EP, Kwekkeboom DJ, Bakker WH, et al. Somatostatin receptor scintigraphy with [111In-DTPA-D-Phe1]- and [123I-Tyr3]-octreotide: the Rotterdam experience with more than 1000 patients. *Eur J Nucl Med.* 1993;20:716-731.

5.   Rufini V, Calcagni ML, Baum RP. Imaging of neuroendocrine tumors. *Semin Nucl Med.* 2006;36:228-247.

6.   Gabriel M, Oberauer A, Dobrozemsky G, et al. 68Ga-DOTA-Tyr3-octreotide PET for assessing response to somatostatin-receptor-mediated radionuclide therapy. *J Nucl Med.* 2009;50:1427-1434.

7.   Buchmann I, Henze M, Engelbrecht S, et al. Comparison of 68Ga-DOTATOC PET and 111In-DTPAOC (Octreoscan) SPECT in patients with neuroendocrine tumours. *Eur J Nucl Med Mol Imaging.* 2007;34:1617-1626.

8.   Krenning EP, Valkema R, Kooij PP, et al. Scintigraphy and radionuclide therapy with [indium-111-labelled-diethyl triamine penta-acetic acid-D-Phe1]-octreotide. *Ital J Gastroenterol Hepatol.* 1999;31 Suppl 2:S219-223.

9.   Kwekkeboom D, Krenning EP, de Jong M. Peptide receptor imaging and therapy. *J Nucl Med.* 2000;41:1704-1713.

10.   Kunikowska J, Królicki L, Hubalewska-Dydejczyk A, Mikołajczak R, Sowa-Staszczak A, Pawlak D. Clinical results of radionuclide therapy of neuroendocrine tumours with 90Y-DOTATATE and tandem 90Y/177Lu-DOTATATE: which is a better therapy option? *Eur J Nucl Med Mol Imaging.* 2011;38:1788-1797.

11.   Maxwell JE, O'Dorisio TM, Howe JR. Biochemical Diagnosis and Preoperative Imaging of Gastroenteropancreatic Neuroendocrine Tumors. *Surg Oncol Clin N Am.* 2016;25:171-194.

12.   Dahdaleh FS, Lorenzen A, Rajput M, et al. The value of preoperative imaging in small bowel neuroendocrine tumors. *Ann Surg Oncol.* 2013;20:1912-1917.

13.   Woodbridge LR, Murtagh BM, Yu DF, Planche KL. Midgut neuroendocrine tumors: imaging assessment for surgical resection. *Radiographics.* 2014;34:413-426.

14.   Sahani DV, Bonaffini PA, Fernández-Del Castillo C, Blake MA. Gastroenteropancreatic neuroendocrine tumors: role of imaging in diagnosis and management. *Radiology.* 2013;266:38-61.

15.   Kuo JH, Lee JA, Chabot JA. Nonfunctional pancreatic neuroendocrine tumors. *Surg Clin North Am.* 2014;94:689-708.

16.   Bushnell DL, Baum RP. Standard imaging techniques for neuroendocrine tumors. *Endocrinol Metab Clin North Am.* 2011;40:153-162, ix.

17.   Worhunsky DJ, Krampitz GW, Poullos PD, et al. Pancreatic neuroendocrine tumours: hypoenhancement on arterial phase computed tomography predicts biological aggressiveness. *HPB (Oxford).* 2014;16:304-311.

18.   Dromain C, de Baere T, Lumbroso J, et al. Detection of liver metastases from endocrine tumors: a prospective comparison of somatostatin receptor scintigraphy, computed tomography, and magnetic resonance imaging. *J Clin Oncol.* 2005;23:70-78.

19.   Yu R, Wachsman A. Imaging of Neuroendocrine Tumors: Indications, Interpretations, Limits, and Pitfalls. *Endocrinol Metab Clin North Am.* 2017;46:795-814.

20.   Shimada K, Isoda H, Hirokawa Y, Arizono S, Shibata T, Togashi K. Comparison of gadolinium-EOB-DTPA-enhanced and diffusion-weighted liver MRI for detection of small hepatic metastases. *Eur Radiol.* 2010;20:2690-2698.

21.   Ba-Ssalamah A, Uffmann M, Saini S, Bastati N, Herold C, Schima W. Clinical value of MRI liver-specific contrast agents: a tailored examination for a confident non-invasive diagnosis of focal liver lesions. *Eur Radiol.* 2009;19:342-357.

22. Qian HF, Zhu YM, Wu X, Li FQ, Xuan HB, Shen J. [Comparison of enhanced magnetic resonance and diffusion-weighted imaging for detection of hepatic metastases]. *Zhongguo Yi Xue Ke Xue Yuan Xue Bao.* 2012;34:621-624.

23. Giesel FL, Kratochwil C, Mehndiratta A, et al. Comparison of neuroendocrine tumor detection and characterization using DOTATOC-PET in correlation with contrast enhanced CT and delayed contrast enhanced MRI. *Eur J Radiol.* 2012;81:2820-2825.

24. Besa C, Ward S, Cui Y, Jajamovich G, Kim M, Taouli B. Neuroendocrine liver metastases: Value of apparent diffusion coefficient and enhancement ratios for characterization of histopathologic grade. *J Magn Reson Imaging.* 2016;44:1432-1441.

25. Kim M, Kang TW, Kim YK, et al. Pancreatic neuroendocrine tumour: Correlation of apparent diffusion coefficient or WHO classification with recurrence-free survival. *Eur J Radiol.* 2016;85:680-687.

26. Hofmann M, Maecke H, Börner R, et al. Biokinetics and imaging with the somatostatin receptor PET radioligand (68)Ga-DOTATOC: preliminary data. *Eur J Nucl Med.* 2001;28:1751-1757.

27. Reubi JC SJ, Waser B, Wenger S, Heppeler A, Schmitt JS, Mäcke HR. Affinity profiles for human somatostatin receptor subtypes SST1-SST5 of somatostatin radiotracers selected for scintigraphic and radiotherapeutic use. *Eur J Nucl Med.* 2000;27:273-282.

28. Poeppel TD, Binse I, Petersenn S, et al. 68Ga-DOTATOC versus 68Ga-DOTATATE PET/CT in functional imaging of neuroendocrine tumors. *J Nucl Med.* 2011;52:1864-1870.

29. Pfeifer A, Knigge U, Binderup T, et al. 64Cu-DOTATATE PET for Neuroendocrine Tumors: A Prospective Head-to-Head Comparison with 111In-DTPA-Octreotide in 112 Patients. *J Nucl Med.* 2015;56:847-854.

30. Johnbeck CB, Knigge U, Loft A, et al. Head-to-Head Comparison of (64)Cu-DOTATATE and (68)Ga-DOTATOC PET/CT: A Prospective Study of 59 Patients with Neuroendocrine Tumors. *J Nucl Med.* 2017;58:451-457.

31. Loft M, Carlsen EA, Johnbeck CB, et al. Cu-DOTATATE PET in Patients with Neuroendocrine Neoplasms: Prospective, Head-to-Head Comparison of Imaging at 1 Hour and 3

Hours After Injection. *J Nucl Med.* 2021;62:73-80.

32.   Hicks RJ, Jackson P, Kong G, et al. Cu-SARTATE PET Imaging of Patients with Neuroendocrine Tumors Demonstrates High Tumor Uptake and Retention, Potentially Allowing Prospective Dosimetry for Peptide Receptor Radionuclide Therapy. *J Nucl Med.* 2019;60:777-785.

33.   Krebs S, Pandit-Taskar N, Reidy D, et al. Biodistribution and radiation dose estimates for (68)Ga-DOTA-JR11 in patients with metastatic neuroendocrine tumors. *Eur J Nucl Med Mol Imaging.* 2019;46:677-685.

34.   Nicolas GP, Schreiter N, Kaul F, et al. Sensitivity Comparison of (68)Ga-OPS202 and (68)Ga-DOTATOC PET/CT in Patients with Gastroenteropancreatic Neuroendocrine Tumors: A Prospective Phase II Imaging Study. *J Nucl Med.* 2018;59:915-921.

35.   Antwi K, Fani M, Heye T, et al. Comparison of glucagon-like peptide-1 receptor (GLP-1R) PET/CT, SPECT/CT and 3T MRI for the localisation of occult insulinomas: evaluation of diagnostic accuracy in a prospective crossover imaging study. *Eur J Nucl Med Mol Imaging.* 2018;45:2318-2327.

36.   Parihar AS, Vadi SK, Kumar R, et al. 68Ga DOTA-Exendin PET/CT for Detection of Insulinoma in a Patient With Persistent Hyperinsulinemic Hypoglycemia. *Clin Nucl Med.* 2018;43:e285-e286.

37.   Werner RA, Weich A, Higuchi T, et al. Imaging of Chemokine Receptor 4 Expression in Neuroendocrine Tumors - a Triple Tracer Comparative Approach. *Theranostics.* 2017;7:1489-1498.

38.   Garin E, Le Jeune F, Devillers A, et al. Predictive value of 18F-FDG PET and somatostatin receptor scintigraphy in patients with metastatic endocrine tumors. *J Nucl Med.* 2009;50:858-864.

39.   Binderup T, Knigge U, Loft A, Federspiel B, Kjaer A. 18F-fluorodeoxyglucose positron emission tomography predicts survival of patients with neuroendocrine tumors. *Clin Cancer Res.* 2010;16:978-985.

40.   Johnbeck CB, Knigge U, Langer SW, et al. Prognostic Value of 18F-FLT PET in Patients with Neuroendocrine Neoplasms: A Prospective Head-to-Head Comparison with 18F-FDG PET and Ki-67 in 100 Patients. *J Nucl Med.* 2016;57:1851-1857.

41. Ezziddin S, Adler L, Sabet A, et al. Prognostic stratification of metastatic gastroenteropancreatic neuroendocrine neoplasms by 18F-FDG PET: feasibility of a metabolic grading system. *J Nucl Med.* 2014;55:1260-1266.

42. Bahri H, Laurence L, Edeline J, et al. High prognostic value of 18F-FDG PET for metastatic gastroenteropancreatic neuroendocrine tumors: a long-term evaluation. *J Nucl Med.* 2014;55:1786-1790.

43. Nilica B, Waitz D, Stevanovic V, et al. Direct comparison of (68)Ga-DOTA-TOC and (18)F-FDG PET/CT in the follow-up of patients with neuroendocrine tumour treated with the first full peptide receptor radionuclide therapy cycle. *Eur J Nucl Med Mol Imaging.* 2016;43:1585-1592.

44. Sansovini M, Severi S, Ianniello A, et al. Long-term follow-up and role of FDG PET in advanced pancreatic neuroendocrine patients treated with (177)Lu-D OTATATE. *Eur J Nucl Med Mol Imaging.* 2017;44:490-499.

45. Hofman MS, Michael M, Kashyap R, Hicks RJ. Modifying the Poor Prognosis Associated with 18F-FDG-Avid NET with Peptide Receptor Chemo-Radionuclide Therapy (PRCRT). *J Nucl Med.* 2015;56:968-969.

46. Miederer M, Seidl S, Buck A, et al. Correlation of immunohistopathological expression of somatostatin receptor 2 with standardised uptake values in 68Ga-DOTATOC PET/CT. *Eur J Nucl Med Mol Imaging.* 2009;36:48-52.

47. Campana D, Ambrosini V, Pezzilli R, et al. Standardized uptake values of (68)Ga-DOTANOC PET: a promising prognostic tool in neuroendocrine tumors. *J Nucl Med.* 2010;51:353-359.

48. Velikyan I, Sundin A, Sörensen J, et al. Quantitative and qualitative intrapatient comparison of 68Ga-DOTATOC and 68Ga-DOTATATE: net uptake rate for accurate quantification. *J Nucl Med.* 2014;55:204-210.

49. Toriihara A, Baratto L, Nobashi T, et al. Prognostic value of somatostatin receptor expressing tumor volume calculated from (68)Ga-DOTATATE PET/CT in patients with well-differentiated neuroendocrine tumors. *Eur J Nucl Med Mol Imaging.* 2019;46:2244-2251.

50. Ambrosini V, Kunikowska J, Baudin E, et al. Consensus on molecular imaging and

theranostics in neuroendocrine neoplasms. *European Journal of Cancer.* 2021;146:56-73.

51.   Shah MH, Goldner WS, Halfdanarson TR, et al. NCCN Guidelines Insights: Neuroendocrine and Adrenal Tumors, Version 2.2018. *J Natl Compr Canc Netw.* 2018;16:693-702.

52.   Öksüz M, Winter L, Pfannenberg C, et al. Peptide receptor radionuclide therapy of neuroendocrine tumors with (90)Y-DOTATOC: is treatment response predictable by pre-therapeutic uptake of (68)Ga-DOTATOC? *Diagn Interv Imaging.* 2014;95:289-300.

53.   Kratochwil C, Stefanova M, Mavriopoulou E, et al. SUV of [68Ga]DOTATOC-PET/CT Predicts Response Probability of PRRT in Neuroendocrine Tumors. *Mol Imaging Biol.* 2015;17:313-318.

54.   Subramaniam RM, Bradshaw ML, Lewis K, Pinho D, Shah C, Walker RC. ACR Practice Parameter for the Performance of Gallium-68 DOTATATE PET/CT for Neuroendocrine Tumors. *Clin Nucl Med.* 2018;43:899-908.

55.   Werner RA, Solnes LB, Javadi MS, et al. SSTR-RADS Version 1.0 as a Reporting System for SSTR PET Imaging and Selection of Potential PRRT Candidates: A Proposed Standardization Framework. *J Nucl Med.* 2018;59:1085-1091.

56.   Hope TA, Calais J, Zhang L, Dieckmann W, Millo C. 111 In-Pentetreotide Scintigraphy Versus 68 Ga-DOTATATE PET: Impact on Krenning Scores and Effect of Tumor Burden *J Nucl Med.* 2019;60:1266-1269.

57.   Werner RA, Bundschuh RA, Bundschuh L, et al. Novel Structured Reporting Systems for Theranostic Radiotracers. *J Nucl Med.* 2019;60:577-584.

58.   Chan DL, Pavlakis N, Schembri GP, et al. Dual Somatostatin Receptor/FDG PET/CT Imaging in Metastatic Neuroendocrine Tumours: Proposal for a Novel Grading Scheme with Prognostic Significance. *Theranostics.* 2017;7:1149-1158.

59.   Werner RA, Thackeray JT, Pomper MG, et al. Recent Updates on Molecular Imaging Reporting and Data Systems (MI-RADS) for Theranostic Radiotracers-Navigating Pitfalls of SSTR- and PSMA-Targeted PET/CT. *J Clin Med.* 2019;8.

60.   Ambrosini V, Campana D, Polverari G, et al. Prognostic Value of 68Ga-DOTANOC PET/CT SUVmax in Patients with Neuroendocrine Tumors of the Pancreas. *J Nucl Med.*

2015;56:1843-1848.

61. Kwekkeboom DJ, Kam BL, van Essen M, et al. Somatostatin-receptor-based imaging and therapy of gastroenteropancreatic neuroendocrine tumors. *Endocr Relat Cancer.* 2010;17:R53-73.

62. Haug AR, Auernhammer CJ, Wängler B, et al. 68Ga-DOTATATE PET/CT for the early prediction of response to somatostatin receptor-mediated radionuclide therapy in patients with well-differentiated neuroendocrine tumors. *J Nucl Med.* 2010;51:1349-1356.

63. Hope TA, Bergsland EK, Bozkurt MF, et al. Appropriate Use Criteria for Somatostatin Receptor PET Imaging in Neuroendocrine Tumors. *J Nucl Med.* 2018;59:66-74.

64. Graf J, Pape UF, Jann H, et al. Prognostic Significance of Somatostatin Receptor Heterogeneity in Progressive Neuroendocrine Tumor Treated with Lu-177 DOTATOC or Lu-177 DOTATATE. *Eur J Nucl Med Mol Imaging.* 2020;47:881-894.

65. Bodei L, Kidd MS, Singh A, et al. PRRT genomic signature in blood for prediction of 177 Lu-octreotate efficacy. *Eur J Nucl Med Mol Imaging.* 2018;45:1155-1169.

66. Bodei L, Kidd MS, Singh A, et al. PRRT neuroendocrine tumor response monitored using circulating transcript analysis: the NETest. *Eur J Nucl Med Mol Imaging.* 2020;47:895-906.

67. Pu N, Habib JR, Bejjani M, et al. The effect of primary site, functional status and treatment modality on survival in gastroenteropancreatic neuroendocrine neoplasms with synchronous liver metastasis: a US population-based study. *Ann Transl Med.* 2021;9:329.

Tables

Table 1: In-vitro affinity (IC_{50} in nmol*) of DOTA-peptides for common SSTR sub-types (*5*)

Radiopeptide†	SSTR-2	SSTR-3	SSTR-5
^{111}In-DOTANOC	2.9	8	11.2
^{111}In-DOTATATE	1.5	>1000	547
^{111}In-DOTATOC	4.6	120	130
^{68}Ga-DOTANOC	1.9	40	7.2
^{68}Ga-DOTATATE	0.2	>1000	377
^{68}Ga-DOTATOC	2.5	613	73

Lower values represent higher affinity. †DOTANOC – DOTA-[1-Nal^3]octreotide; DOTATATE – DOTA-[Tyr^3]octreotate; DOTATOC – DOTA--[Tyr^3]octreotide.
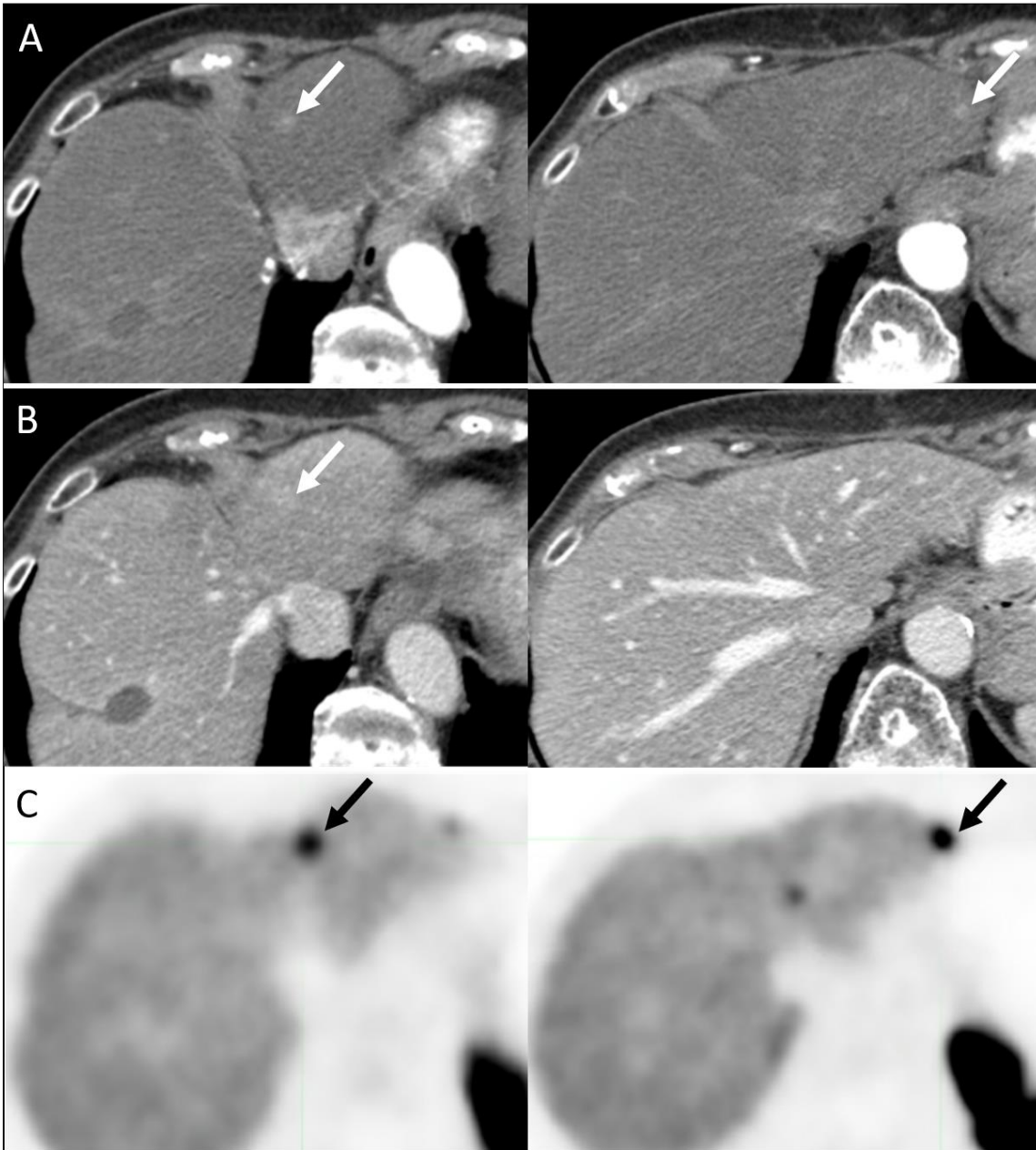
Figure 1. Pancreatic NEN with hepatic metastases. A - Abdominal CECT showing two small arterially enhancing left hepatic lesions. B - corresponding portal venous phase, where the lesions are more inconspicuous. C - trans-axial PET images showing ^{68}Ga-DOTATATE avidity in the same lesions.
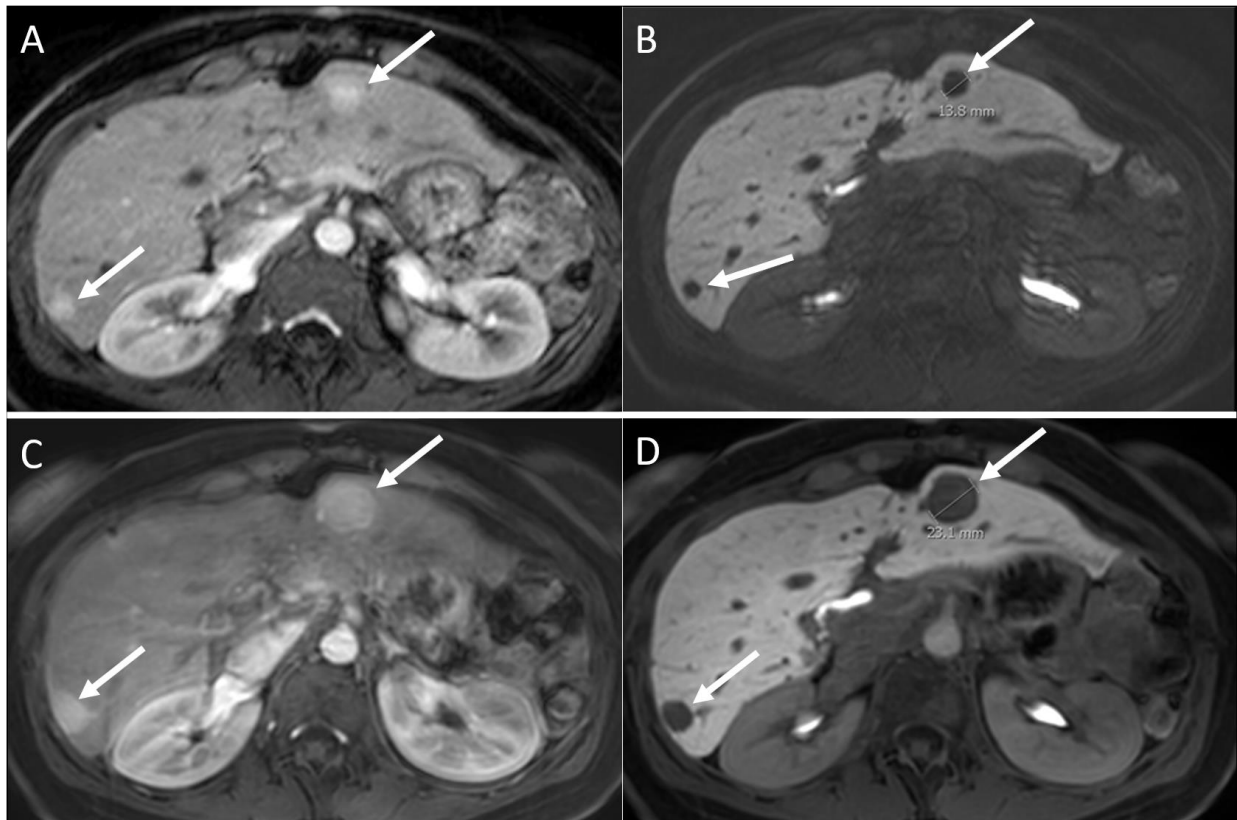
Figure 2. Abdominal CEMRI (with Gadoxetate disodium) in a patient with pancreatic NEN with hepatic metastases. Arterial phase (A) and 20-minute delayed-phase (B) images: the two metastatic lesions (arrows) show arterial enhancement and contrast washout on the delayed phase. Arterial phase (C) and delayed-phase (D) images showing the increased size of the previous lesions on an 18-month follow-up MRI. The lesions are better delineated on the delayed phase facilitating accurate size measurements.
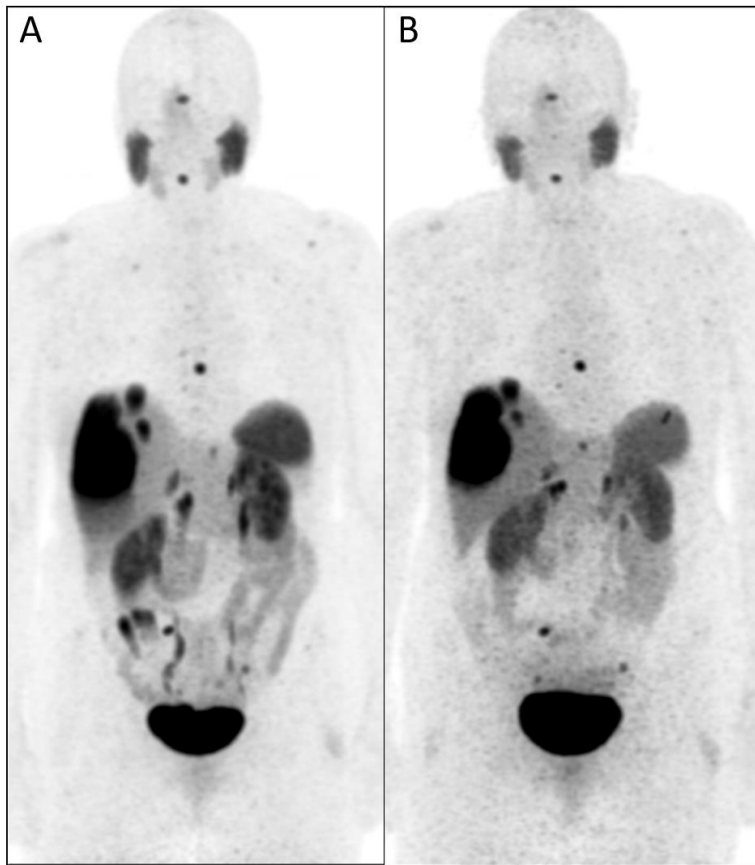
Figure 3. ^{68}Ga-DOTATATE (A) and ^{64}Cu-DOTATATE (B) PET imaging of metastatic NEN showing similar findings on the maximum intensity projection images. Both the studies were performed as part of PET/MRI, with uptake times for ^{68}Ga-DOTATATE, and ^{64}Cu-DOTATATE being 113 minutes, and 118 minutes, respectively (3 minutes/ bed position for both).
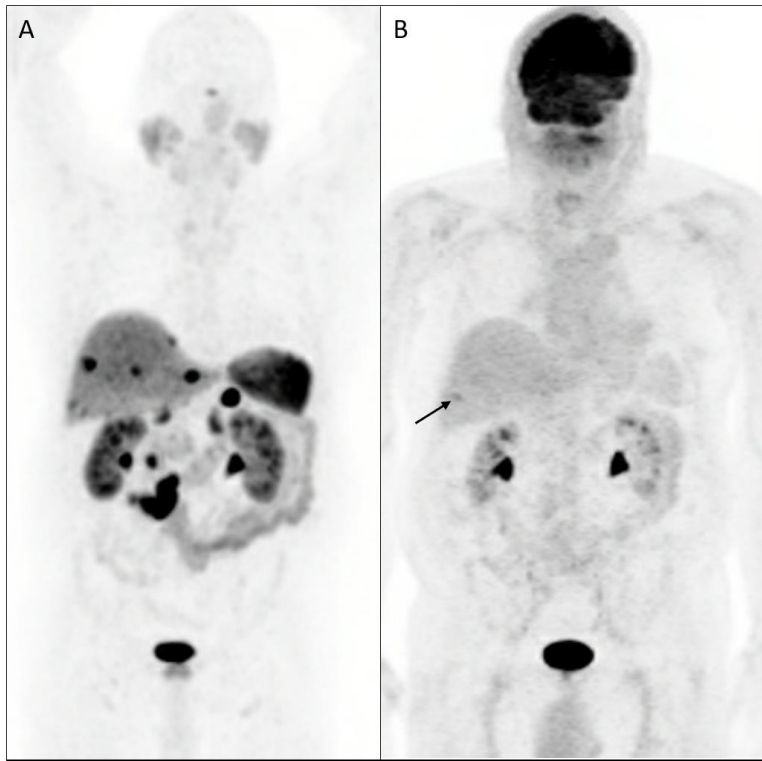
**Figure 4**. Maximum intensity projection images of a patient with metastatic Grade-1 (Ki67 <2%) NEN from a small-bowel primary. ^{68}Ga-DOTATATE PET (A) shows prominent uptake in the primary tumor, lymphadenopathy, and liver metastases. ^{18}F-FDG PET (B) shows no abnormal uptake (arrow - incidentally noted fractured rib).
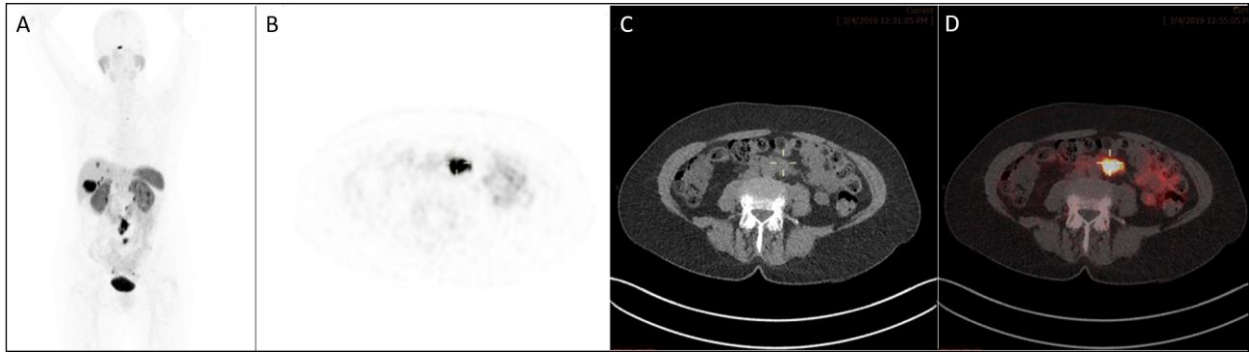
Figure 5. 60-year-old woman with small bowel NET on Octreotide therapy. ^{68}Ga-DOTATATE PET/CT (A-MIP, trans-axial PET–B, CT–C, fused PET/CT-D) shows prominent uptake in the tumor sites. This would make her eligible for PRRT but the overall limited extent of disease in the liver and retroperitoneum favors surgical resection over PRRT.
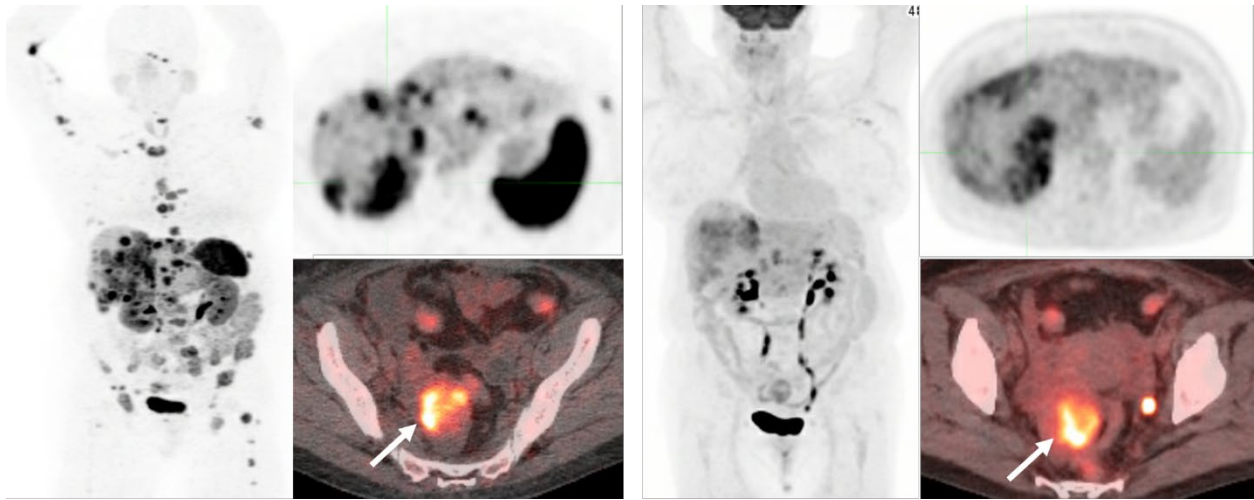
Supplementary Figure 1. MIP and trans-axial PET and fused PET/CT images of a patient with metastatic Grade-3 (Ki67 50%) well-differentiated pancreatic NET. ^{68}Ga-DOTATATE PET (left) shows prominent uptake in the primary tumor and extensive liver and osseous metastases. ^{18}F-FDG PET (right) shows mild-to-moderate uptake in the primary tumor and liver metastases, with no uptake in additional liver and extensive osseous metastases. A right ovarian metastasis (arrow) shows uptake with both tracers.
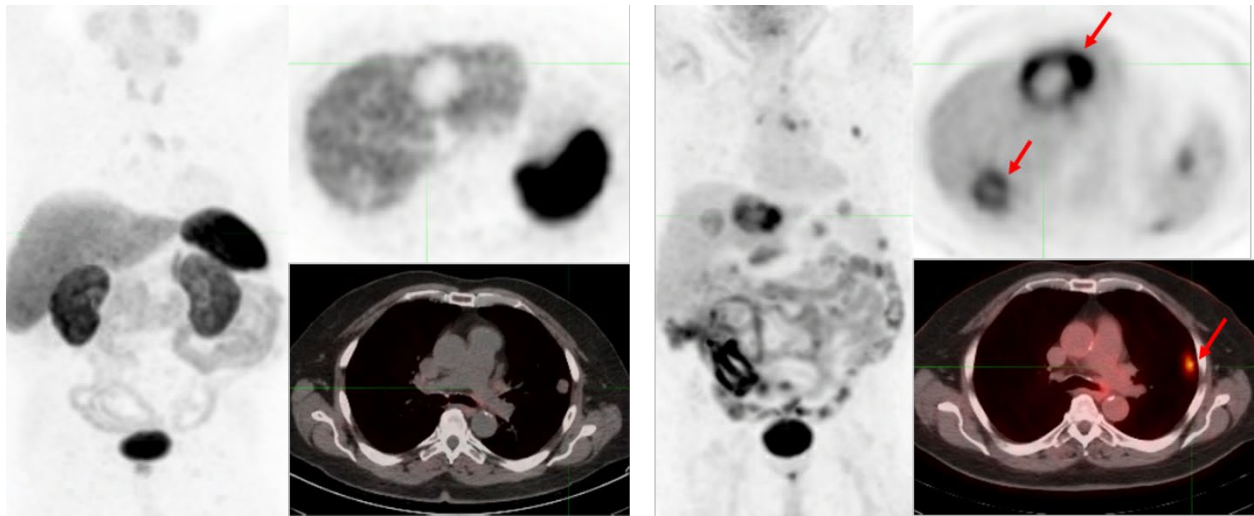
Supplementary Figure 2. MIP and trans-axial PET and fused PET/CT images of a patient with metastatic high-grade large-cell pulmonary neuroendocrine carcinoma. ^{68}Ga-DOTATATE PET (left) shows no abnormal uptake. ^{18}F-FDG PET (right) shows uptake in the primary lung tumor as well as nodal, liver, and splenic metastases.
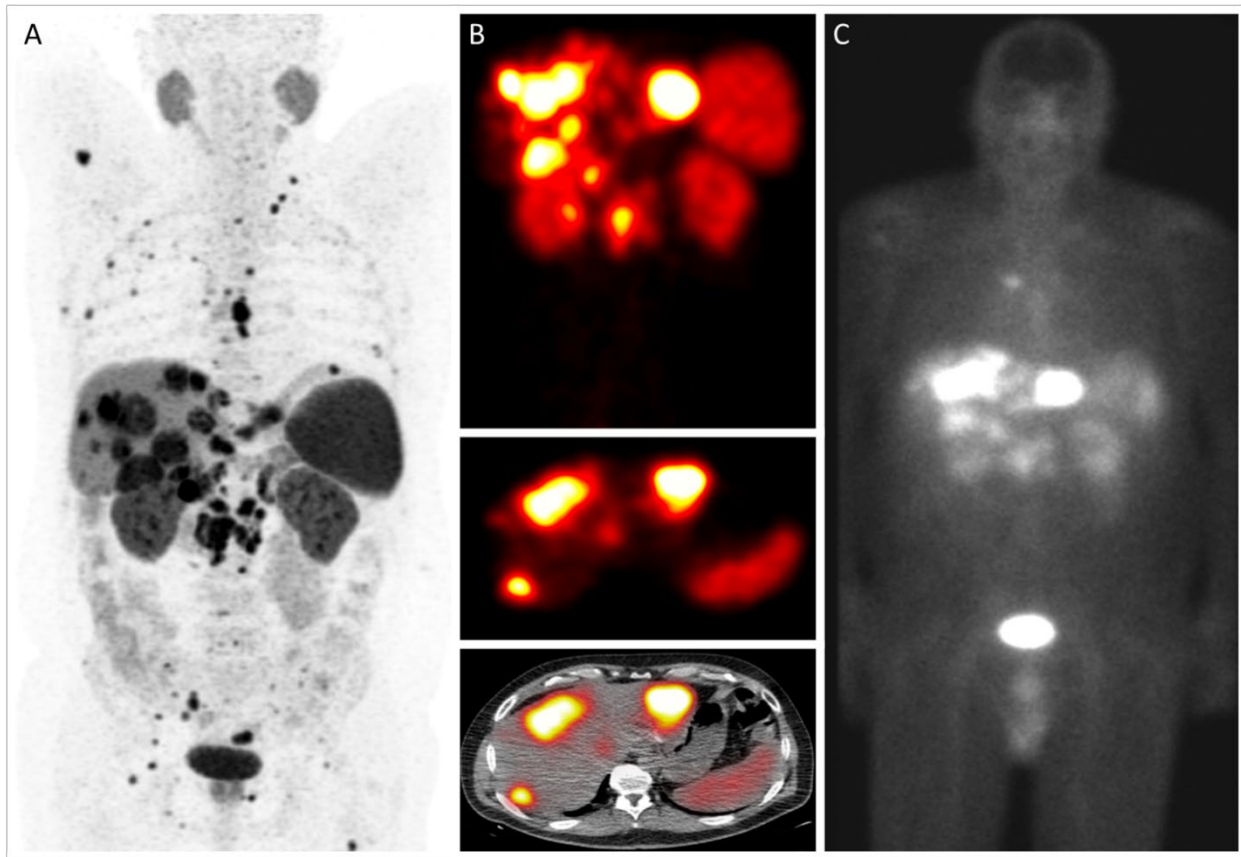
Supplementary Figure 3. Comparison of ^{68}Ga-DOTATATE PET and ^{111}In-Pentetreotide. The higher resolution of PET (A) allows for visualization of additional lesions than planar scintigraphy (C) or SPECT/CT (B). This may result in smaller lesions having a higher Krenning score. However, as this example shows, all imaging modalities show an overall Krenning score of 5 for this patient. Reprinted with permission from *JNM*. Hope TA et al. J Nucl Med. 2019;60:1266-1269.

EXAMINATION: ^{68}Ga-DOTATATE PET/CT IMAGING

DATE OF STUDY: 01/01/0001

SCANNER: ABC

RADIOPHARMACEUTICAL: 5.2 mCi ^{68}Ga-DOTATATE i.v. Injection site: Left antecubital

HISTORY: Incidentally detected hyper-enhancing pancreatic uncinate process mass on CECT – underwent endoscopic biopsy 1 month back, with pathology showing Grade-2, well-differentiated neuroendocrine tumor (Ki-67: 5.9%). Chromogranin A levels are elevated (128 ng/mL; normal: < 93 ng/mL). The study is requested for initial staging.

TECHNIQUE: After intravenous administration of ^{68}Ga-DOTATATE, non-contrast CT images were obtained for attenuation correction and for fusion with emission PET images to allow for anatomical localization of PET findings. Emission PET images were then obtained. The study was interpreted on the XYZ workstation.

Scanned area: Skull vertex to the proximal thighs; the time from injection of tracer to start of imaging for this scan position was 71 minutes.

COMPARISON: Outside hospital CT chest abdomen pelvis dated 02/02/0001

FINDINGS:
Markedly tracer-avid mass in the pancreatic head measuring 4.0 x 3.0 cm in axial dimensions with a SUVmax of 53.5 (axial image #222). No other focus of pathologic tracer avidity in the pancreas.

There is a 0.7 cm markedly tracer-avid peripancreatic/ pericaval lymph node just anterior to the right renal vein with SUVmax of 38.2 (axial image #333).

No other focus of pathologic tracer avidity in the rest of the whole-body survey.

Additional CT FINDINGS: Calcified hilar mediastinal lymph nodes from old granulomatous disease. Scattered calcified granulomas in the lungs. Coronary artery atherosclerotic disease.

IMPRESSION:
1. Markedly ^{68}Ga-DOTATATE avid mass in the pancreatic head consistent with the patient's biopsy-proven well-differentiated neuroendocrine tumor.

2. ^{68}Ga-DOTATATE avid caval lymph node consistent with site of locoregional nodal spread. No ^{68}Ga-DOTATATE PET evidence of distant metastatic disease.

Dictated by:

Electronically signed by:

Supplementary Figure 4. Standardized reporting for ^{68}Ga-DOTATATE PET in a patient with NET.